New Nitride-Based Devices for Electrical Detection of DNA Hybridization

by

Ryan Taylor Sheffler

Submitted to the Department of Physics
in partial fulfillment of the requirements for the degree of

Bachelor of Science

at the

MASSACHUSETTS INSTITUTE OF TECHNOLOGY

June 2007

Author .....
Department of Physics
May 11, 2007

Certified by .....
Professor Tomas Palacios
Department of Electrical Engineering and Computer Science
Thesis Supervisor

Accepted by .....
Professor David E. Pritchard
Senior Thesis Coordinator, Department of Physics

New Nitride-Based Devices for Electrical Detection of DNA Hybridization

by

Ryan Taylor Sheffler

Submitted to the Department of Physics
on May 11, 2007, in partial fulfillment of the
requirements for the degree of
Bachelor of Science

Abstract

In this thesis we designed and began the fabrication of three new solid state sensors for the detection of DNA hybridization through electrical measurements. The first sensor is a surface acoustic wave device with tapered IDTs capable of giving us a tomographic image of the functionalized sensor surface. We investigated using an array of these type sensors to produce a novel DNA sequencing platform on par with the state-of-the-art sequencing machines of today. The second sensor we designed is a quantum dot-based conduction sensor, where quantum dots in the substrate exponentially increase its conductivity when hybridization events occur. The third sensor is a HEMT AlGaN transistor where the drain access region serves as the functionalized area, so hybridization events increase the parasitic capacitance and change the switching frequency of the device. We have also identified the sensitivity limits and other relevant parameters for each of these devices.

Thesis Supervisor: Professor Tomas Palacios
Title: Department of Electrical Engineering and Computer Science

Acknowledgments

The author would like to acknowledge Tomas Palacios for his help and support throughout this project, without his ideas and enthusiasm none of this would have been possible. The author would also like to thank Xu Zhao and Will Chung, two graduate students in Prof. Palacios's group who were incredibly generous with their time all semester and very helpful in the cleanroom. And finally the author would like to thank Dennis Ward for actually making the photolithographic mask, as well as Paul Tierney and Dave Terry for the training on the complex fabrication equipment.

THIS PAGE INTENTIONALLY LEFT BLANK

Contents

List of Figures

Chapter 1

Introduction

1.1 The Importance of DNA in Living Organisms

Life here on earth has a fundamental dependence on organic chemistry. The laws of quantum physics allow molecules and compounds based around the carbon atom to be built up into the very complex chemical structures that living organisms need in order to exist. There are four general classes of organic compounds; amino acids which are the building blocks of proteins; carbohydrates which include sugar, starch and cellulose; lipids which include fats and hormones, and finally nucleic acids which include DNA and RNA [1]. It is within the intricate structure of this last class of compounds that the information processing necessary to construct an organism and to orchestrate its functioning is carried out.

Deoxyribonucleic acid (DNA) is, in fact, the fundamental hereditary material that directs the development and functioning of all living organisms. It is like a blueprint, in some sense, because it provides long-term storage for the information needed to construct the building-blocks of an organism. It is also the DNA that passes on genetic information to the next generation, and that by making rare mistakes, sets the conditions for evolution by natural selection. The identification and characterization of DNA as the material of heredity is one of the greatest scientific breakthroughs of the twentieth century and its implications are overwhelming.

Today we know that DNA is a long polymer made of repeating units called nu-

cleotides. The four types of nucleotides - also called bases - are: adenine, thymine, guanine, and cytosine. In nature DNA typically exists not as a single molecule, but as two closely associated molecules wound together in a double helix. The two strands of DNA bind together because their nucleotides have a very specific attraction for one another known as complementary base pairing. Adenine bonds with thymine; guanine bonds with cytosine. Therefore, two single strands of DNA will join together only if their nucleotide sequences are arranged to allow this base pairing to occur. Chapter two describes the structure and properties of DNA in more detail.

Genes are long sequences of DNA base pairs that encode information about things like our eye color, our hormone levels, and our likelihood to develop cancer. The human genome, for example, contains about 25,000 genes and six billion individual nucleotides. In order to discover and classify genes, we need a way to read the exact base pair pattern present in our DNA. Current methods are slow and expensive; sequencing a human genome today costs approximately $20 million and takes several years [2]. But because there is so much benefit to mankind if we can sequence genes very quickly and very cheaply, there is a general level of dissatisfaction among many in the field with regard to the rate of progress on sequencing techniques. To stimulate the technology, in October of 2006 the X-Prize Foundation announced a $10 million dollar award for producing highly accurate sequences of 100 human genomes in 10 days or less without spending more than $10,000 per genome [3].

The next-generation sequencing projects will be able to sequence the entire human genome in a matter of months for around $1 million [2]. Those projects will use several sequencing machines in parallel, each of which uses a gel-electrophoresis system that can run 64 samples (each 500 base-pairs in length) over an 8 hour period [33], effectively sequencing 320,000 base pairs per day per machine. In order to improve this number even further, researchers are looking for ways to run more reactions in parallel, reduce the preparation/clean-up time, and even speed up the sequencing reaction itself [33].

The ultimate goal of many researchers is the so-called "$1,000 genome," the point at which DNA sequencing becomes affordable enough that individuals might deem

it worthwhile to have a full personal genome sequence appended to their medical records [2]. The applications of such ultra-low-cost sequencing technology would be tremendous:

- Predictive Medicine - geneticists could anticipate an individual's susceptibility to a certain disease or medical condition [2].
- Personalized Medicine - an individual's genetic information could be used to help determine the most effective drug type and dosage [4].
- Gene Expression Profiling - the ability to determine, in real-time, which genes are expressed in a particular cell type at a particular time [4].
- Genotype-Phenotype Associations - so many genomes would allow for rapid hypothesis testing of which genes control which physical traits [4].
- Improved Geneology - quicker analysis and discovery of an organisms lineage [2].
- Pathogen Detection - easier and faster identification/characterization of unknown viruses, bacteria, and other harmful pathogens [4].
- DNA computing - manipulating DNA libraries to carry out highly parallel computations [4].

1.2 Optical Detection of DNA Hybridization

DNA sequencing requires a sensor that can detect the subnanometer-scale differences between the four nucleotides, and most strategies try to exploit the specificity of DNA hybridization to carry out this task. DNA hybridization is the process of combining complementary, single-stranded DNA fragments into the double-helix structure found in nature. Since base pairing is highly specific, the two strands of DNA have to be perfect complements of each other for hybridization to take place. Therefore,

hybridization allows scientists with DNA strands of a known base sequence to probe the nucleotide sequence of an unknown segment of DNA.

One drawback, however, is that hybridization events are not easy to observe. Most current approaches use an optical detection method based on fluorescently tagging the probe which is expensive, slow and not very sensitive [4]. In fact detecting a single fluorescent molecule is so challenging that multiple instances of the matching reaction must happen at the same time for the optical signal to be strong enough to read [2]. Fortunately a technology known as DNA microarrays have been developed that allow us to vastly multiplex the reactions and speed-up the sequencing process. Figure 1-1 shows how a DNA microarray can be used to quickly identify a particular nucleotide sequence [5].

1.3 Electronic Detection of DNA Hybridization

1.3.1 Advantages of Electronic Detection

Despite the ability to run highly multiplexed reactions with microarrays, sequencing technology based on optically detecting fluorescent tags still requires too many processing steps and costs too much money. In order to circumvent this bottleneck, we have developed three new solid state sensors that can electronically detect a DNA hybridization event.

Shifting from optical detection schemes to electronic detection schemes allows us to leverage all the time, money and cutting edge technology that has poured into the semiconductor industry over the past few decades. Semiconductor devices are sophisticated, fast, small, run on low power, easily mass produced, and extremely cheap. Plus integrating the sensor itself onto an electronic chip allows us to use signal processing techniques that were developed for other applications. The end result is that our new sensors will be able to provide more sensitivity, selectivity, speed, and reliability than current sequencing techniques at a lower cost.

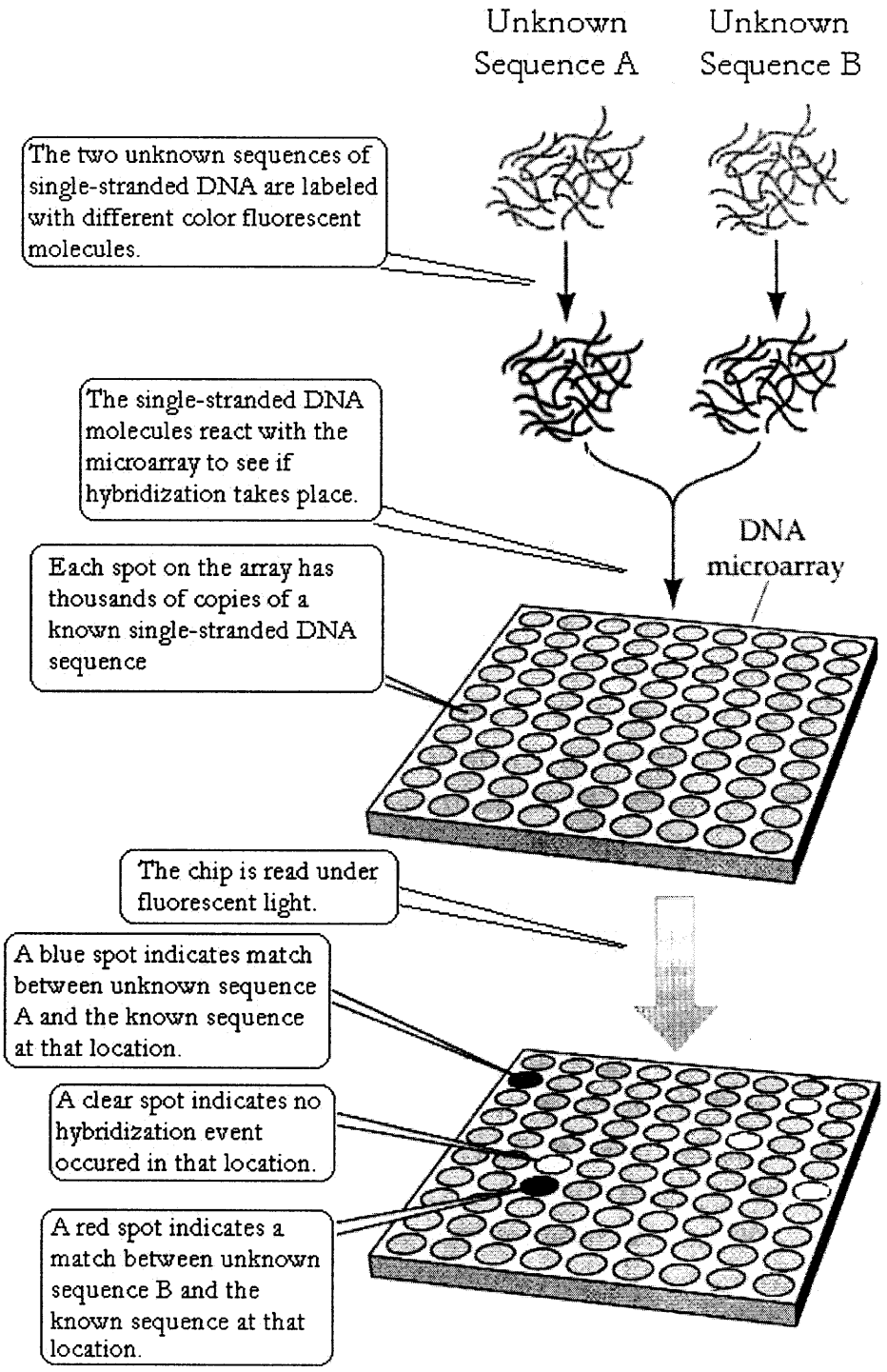

Figure 1-1: Gene sequencing with a DNA microarray. Adapted from [5].

1.3.2 New Electronic Sensors

We worked on three novel electronic sensors. The first is a surface acoustic wave (SAW) tomographic sensor where mass changes on the sensor surface shift the resonant frequency of the structure. The commercial applications of SAW devices as sensors have been limited by the difficulty in achieving high selectivity, since unwanted particles on the surface of the sensor introduce unwanted noise into the output signal. We use a novel approach to overcome this obstacle by using an array of tapered SAW devices as our sensor. These tapered SAW structures will allow us to produce a two-dimensional tomographic image of the sensor surface, increasing the specificity of the detector by helping us discard artifacts in the output signal. Chapter three describes the design of our SAW devices.

The second device is a quantum dot-based conductivity sensor, where the successful hybridization of DNA changes the net surface charge and depletes the carrier density in GaN quantum dots that have been grown immediately below the surface. The change in carrier density should be detectable as a change in conductivity between two nearby ohmic contacts. Chapter four describes the design of our quantum dot-based conductivity sensors.

The third device is a parasitic-capacitance transistor-based sensor where the drain acess region of an AlGaN/GaN high electron mobility transistor (HEMT) has been functionalized to allow the hybridization of DNA molecules. As hybridization events alter the charge on the surface of the sensor, the parasitic capacitance between the gate and the drain will change as well, which we detect as a shift in the frequency and pulsed i-v performance of the device. Chapter five describes the design of our transistor-based sensors.

The ultimate goal of this project is to lay the groundwork for a novel electronics-based genetic analysis platform. Towards this goal, we have designed and begun fabrication of these three DNA hybridization sensors.

Chapter 2

Materials and Fabrication

2.1 Properties of DNA

2.1.1 Molecular Structure of DNA

DNA is a long polymer of nucleotides, each consisting of a molecule of the sugar deoxyribose, a phosphate group, and a nitrogen-containing base. The only differences between the four nucleotides that make-up DNA are their nitrogeneous bases. The structure of a nucleotide is illustrated in Figure 2-1 [6].

The molecular structure of DNA can be summarized best by its four key features, all illustrated in Figure 2-2:

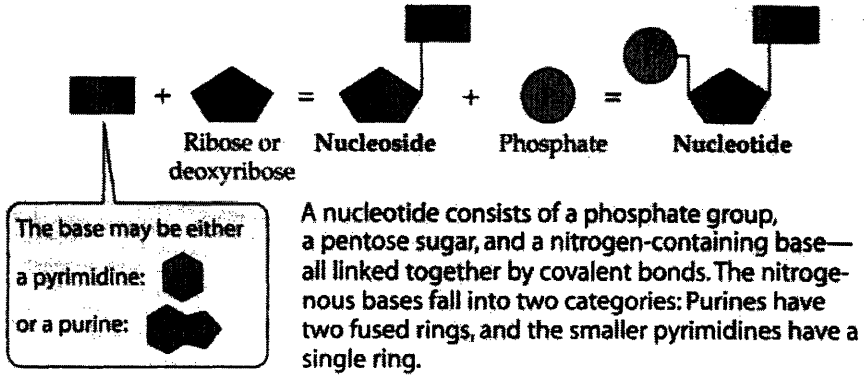

Figure 2-1: Structure of the four nucleotide bases that make-up DNA. From [6].

- Double-stranded helix - the sugar-phosphate backbone of the two DNA strands coil around the outside of the helix and allow the nitrogenous bases to point towards the center of the molecule, where complementary base pairing between adenine (A) - thymine (T) and cytosine (C) - guanine (G) occurs via hydrogen bonding [7].

- Uniform Diameter - The AT and GC pairs are geometrically structured so that they are of equal length, allowing them to fit in between the sugar-phosphate backbones like rungs on a ladder. As a result the DNA molecule has a uniform diameter of about 2 nm [7].

- Right-Handed - the helix of the DNA twists according to the familiar right-hand rule [7].

- Antiparallel Strands - the sugar-phosphate backbones have some directionality because of how they link adjacent nucleotides. Phosphate groups connect the 3' carbon of one deoxyribose molecule to the 5' carbon of the next to link successive sugars together. The prime designates the position of a carbon atom in the five-carbon sugar deoxyribose. The DNA molecule is structured so that the two strands run in opposite directions [7].

DNA's molecular makeup is essential to its function as genetic material. The double-helix enables complementary base-pairing and promotes a stable molecule capable of providing long-term storage of an organisms genetic information. The genetic information is easily replicated and passed to offspring as a result of complementary base pairing. Also important is the fact that the information stored is subject to permanent change through mutation - an alteration of the nucleotide sequence - which allows evolution to occur [7].

2.1.2 Mass, Charge, and Stiffness of DNA

Heating a sample of DNA will cause it to denature - meaning all the hydrogen bonds between nucleotides disappear and the double-helix structure unravels [7]. This de-

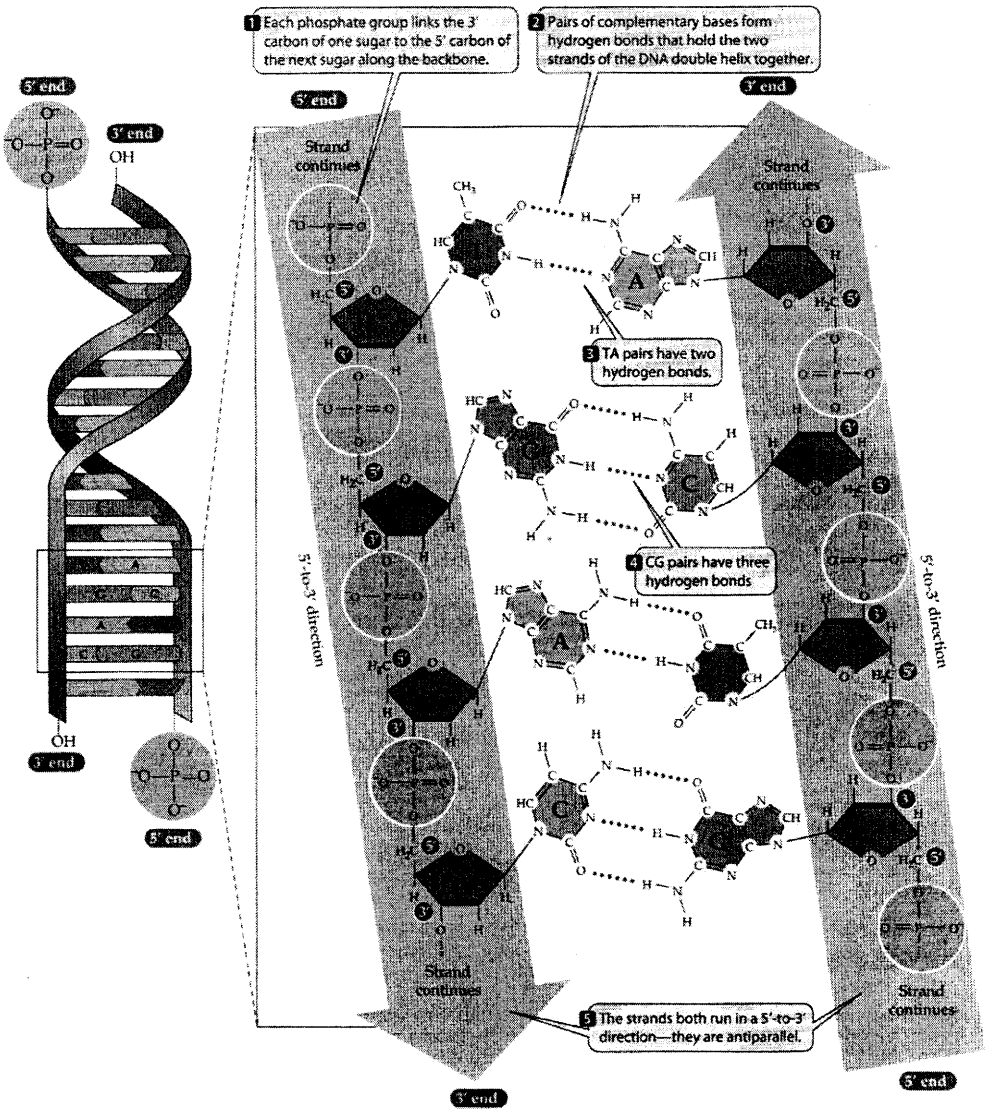

Figure 2-2: Molecular Architecture of DNA. From [7].

naturing creates single-stranded DNA, or dehybridized DNA. Our sensors rely on the different physical properties of single-stranded and double-stranded DNA to detect hybridization. As an example, we know that a double-stranded DNA molecule that is 1578 base-pairs long will have a mass of $1.6\text{x}10^{-18}$ g [11]. This means that the density of a double-stranded DNA molecule is about $1\text{x}10^{-21}$ g / base-pair, and single-stranded DNA will have a density of approximately half that number.

Each strand of DNA is negatively charged at neutral pH because of the phosphate groups on its helical backbone [7]. Therefore double-stranded, hybridized DNA will have twice the negative charge as a similar size piece of single-stranded, dehybridized DNA. We also know that since there is exactly one phosphate group - with one extra electron - per nucleotide, double-stranded DNA will have a negative charge of 2 e^- / base-pair.

Single and double-stranded DNA also differ in their stiffness, or how strongly they resist being stretched beyond their normal lengths. Resistance to such stretching can be characterized by an elastic stretch modulus, S [12]. Although S values vary quite a bit depending on environmental conditions, a typical S value is 1000 pN for double-stranded DNA [14] and 300 pN for single-stranded DNA [13]. Double-stranded DNA is almost three times stiffer than single-stranded DNA.

2.2 Nitride Semiconductors

We choose to work with nitride semiconductors (mainly GaN) for this project because they have a number of very nice properties that make them ideal candidates for biosensors:

- Chemically very stable, even without complicated passivation technology [27].
- Non-toxic to living cells [27].
- Transparent to visible light, opening the door for multifunctional optoelectronic sensors [27].
- Able to operate at high temperatures [26].

- Piezoelectric, making them good candidates for acoustic wave sensors [21].

2.3 Surface Functionalization

Nitride-based devices are well-suited for bioelectronic applications because they are nontoxic and chemically stable under physiological conditions [27], but we still need a reliable method for covantly attaching specific biomolecules to the surface of our devices. We have chosen to use SupraMolecular NanoStamping (SuNS) to functionalize the surface of our sensors with single stranded DNA molecules. SuNS is a method, developed by Professor Francesco Stellacci at MIT, that can be used to immobilize and pattern DNA molecules with high resolution onto a substrate. The technique has already been successfully demonstrated with 100 nm resolution on silicon [8], and we will use a similar technique to functionalize the nitride semiconductor surfaces of our sensors.

The SuNS method consists of stamping a DNA pattern from one substrate to another via a hybridization/contact/dehybridization cycle. The procedure is as follows [8]:

1. Pattern a self-assembled monolayer (SAM) of single-strand-DNA terminated molecules onto the master substrate by spotting or dip pen lithography.

2. Hybridize complement strands to the single-strand-DNA patterned on the surface of the master. The complement strands should be functionalized - on the end far away from the master substrate - with a chemical moiety capable of reacting with the surface of our nitride semiconductor.

3. Bring a second substrate (in this case our nitride semiconductor) close to the first so that chemical bonds can form between the reactive group on the complement DNA and the nitride surface.

4. Apply heat (40 - 60 degrees C depending on DNA length) to denature the hydrogen bonds of the double helix, and separate the two substrates.

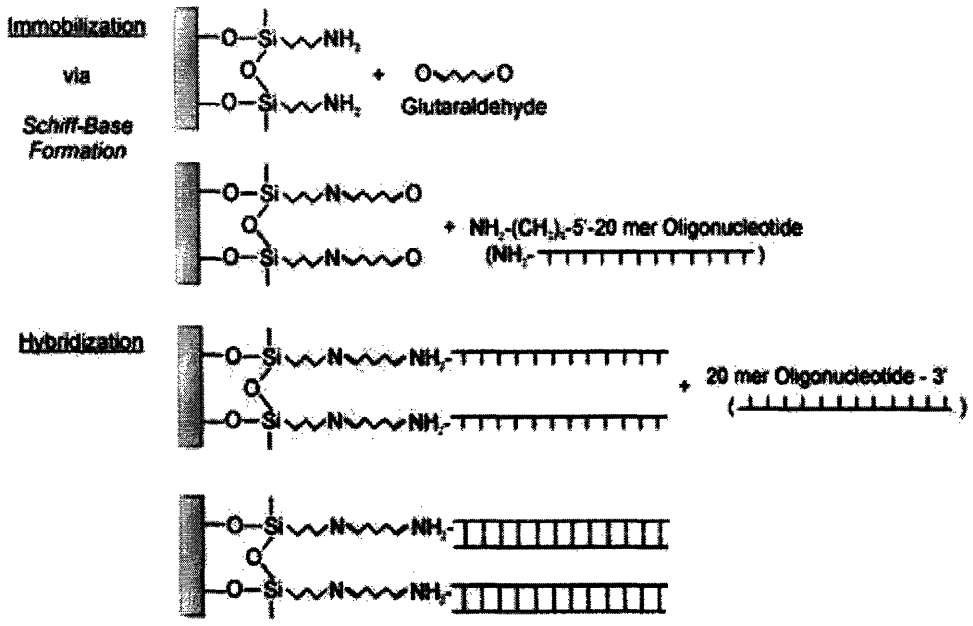

Figure 2-3: Schematic of APTES-SAM formation on hydroxylated GaN and subsequent immobilization of DNA by Schiff-Base formation. From [9].

The primary advantages of the SuNS method are that a single master can be used repeatedly for printing onto various surfaces, and that the surface can be functionalized with a large number of different molecules simultaneously.

Since SuNS has never been used to pattern DNA onto nitride substrates before, we still need to develop the chemistry that will covalently attach the complement strands to the nitride surface, and in doing this we will take advantage of the fact that aminopropyltriethoxysilane (APTES) molecules form SAMs on hydroxylated GaN surfaces [9]. APTES molecules are particularly useful for our application because their active amino group is perfectly suited for immobilizing biomolecules like DNA [9]. We plan to attach DNA molecules to the APTES SAM by a reaction known as Schiff-Base formation, depicted in Figure 2-3.

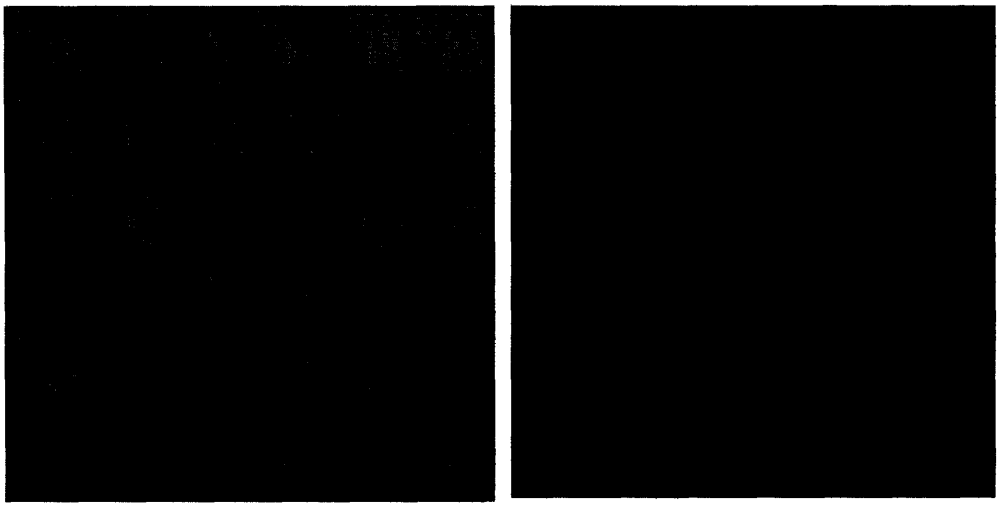

Figure 2-4: Layout of entire mask (left) and a unit cell (right).

2.4 Fabrication

2.4.1 Mask Design

We designed the photolithographic mask for this sensor project so that we could conduct a first-pass, proof-of-concept type experiment. We wanted to compare the sensitivity of our new sensors with the current technologies and lay out structures that would allow us to perform some of the basic optimizations that we have anticipated in our design.

Our mask has a unit cell that is approximately 1 cm by 1 cm so that it matches the samples on which we plan to fabricate these devices. An image of the unit cell is shown on the right in Figure 2-4. Each unit cell contains several of each type of sensor. The entire mask is a 6x6 grid of these unit cells that is shown on the left in Figure 2-4. Our mask has three layers:

- Shottky metal layer
- Ohmic contact layer
- Isolation layer

The Schottky metal layer (in green) is what defines the electrodes on our SAW devices, the gates on our transistors, and the center part of the Shottky diodes. The ohmic

contact layer (in red) defines the connection pads for our conductivity sensors, the source and drain on our transistors, and the outer portion of the Shottky diodes. Finally the isolation layer (in yellow) separates the conductivity sensors and the active regions of the transistors from the rest of the substrate so nothing outside of that region can contaminate the signal.

2.4.2 Processing

We perform our processing in the Technology Research Laboratory (TRL), a part of MIT's Microsystems Technology Laboratories (MTL). The general processes that we use to create the devices are: cleaning, photolithography, metallization, annealing, and etching.

We clean our wafers by rinsing them first with acetone to remove any organic molecules on the surface of the wafer. Then we rinse the wafers with isopropanol to remove the acetone, and finally we rinse with DI water to remove the isopropanol. In the final device fabrication, we plan to use the ultrasonic cleaning equipment to perform these rinses.

We use the following photolithography recipe to coat our wafers with 1.4-1.5 μm of photoresist. We found that the baking and exposure times give us a good crisp image of our mask in the photoresist after development. The procedure is:

1. HMDS
2. AZ5214 Image Reversal Photoresist - coat 6 seconds at 500 rpm, spread 8 seconds at 750 rpm, and spin 30 seconds at 4000 rpm.
3. Prebake 1 minute at 110 degrees C.
4. 30 second exposure with patterned mask.
5. Postbake 2 minutes at 125 degrees C.
6. 500 second exposeure with clear flood mask.
7. Develop for 2.5 minutes and then rinse with DI water.

We use the ebeamAU machine in TRL to perform metallization. For the Schottky layer, we put down 200 $\AA$ of Ni, 600 $\AA$ of Au and a final 200 $\AA$ of Ni via ebeam evaporation. We use an overnight soak in acetone followed by an ultrasonic rinse in acetone/isopropanol/water to perform the liftoff.

Unfortunately we have not been able to go any further in the fabrication process, but we anticipate successful fabrication of at least the SAW devices within the next few weeks.

THIS PAGE INTENTIONALLY LEFT BLANK

Chapter 3

Surface Acoustic Wave Tomographic Sensor

Our first device that we will use to detect DNA hybridization is a surface acoustic wave (SAW) sensor like the one shown in Figure 3-1. The oscillating voltage applied to the input electrodes (IDTs) creates waves in the surface of the material that propagate across the device until they are detected by the output electrodes. When this type of device is used as a biosensor, the surface between the input and output IDTs is functionalized to allow binding of the molecule of interest. The way the acoustic waves interact with the bound molecules provides the sensing mechanism. This chapter explains the operational principles of these devices, design considerations, as well as some of the enhancements we have made to their basic design.

3.1 Wave Propagation in Solids

Solids are an elastic medium that behave much like a distributed mass-spring system in the sense that a disturbance of a single part will propagate throughout the entire structure. These disturbances can be thought of as waves, and the type of wave we are most concerned with are the Rayleigh surface waves depicted in Figure 3-2. Rayleigh waves have velocities ranging from 2000 - 8000 m/s depending on the material [15]. For GaN, Rayleigh surface waves have $v_0 = 3700$ m/s [21].

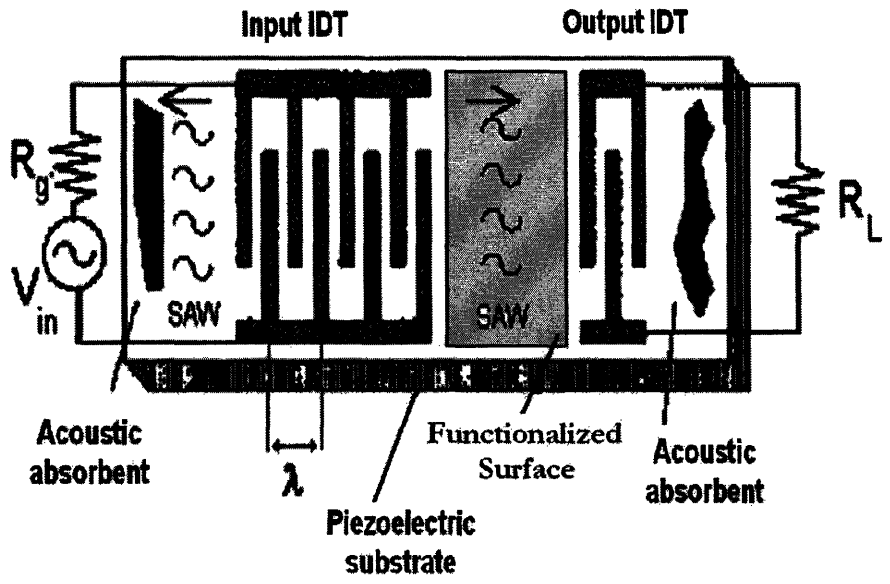

Figure 3-1: Basic SAW Sensor.

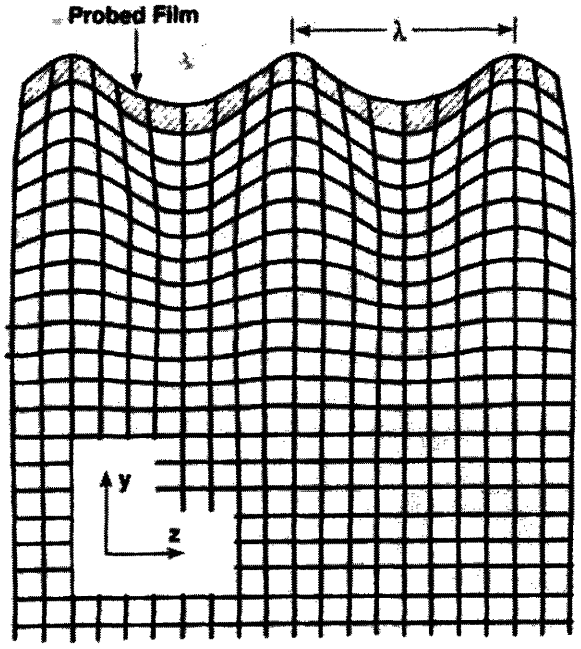

Figure 3-2: Rayleigh surface wave propagating through a solid. From [17].

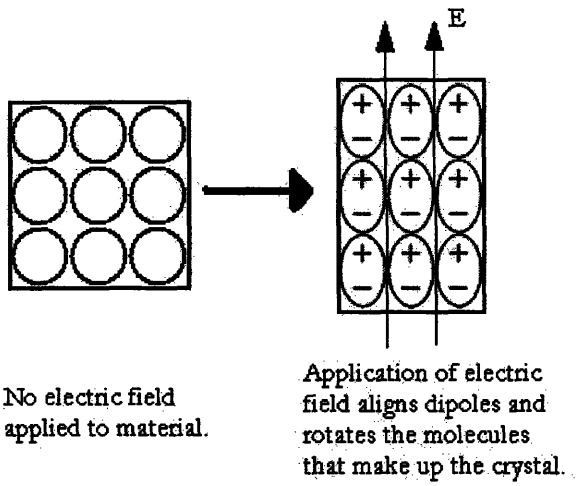

Figure 3-3: Piezoelectric Phenomenon.

3.2 Piezoelectricity

Piezoelectricity is the coupling between the mechanical and electrical properties in a solid such that the application of an electric field to the material can actually induce mechanical stress. From a molecular standpoint, piezoelectricity results when an electric field is applied to a group of dipoles and causes them to actually rotate within the crystal lattice [16]. The rotation can actually change the conformation of the molecules that make-up the crystal and distort its size as shown in Figure 3-3. Piezoelectricity occurs when the crystal structure of the material lacks a center of inversion symmetry, so there is also a reverse piezoelectric effect which occurs when a mechanical disturbance rearranges the charges in a crystal such that a net, macroscopic, electrical polarization results [16].

Piezoelectric materials are characterized by their electromechanical coupling coefficient K^2, which captures the ratio of peak eletrical energy to peak strain energy [16]. Basically, it is a measure of how efficiently the material converts an an electrical disturbance into a mechanical deformation of the crystal structure. The nitride semiconductors we will be using for our devices have particularly high electromechanical coupling coefficients ($K^2 = 4.2\%$), especially for a semiconductor material [21].

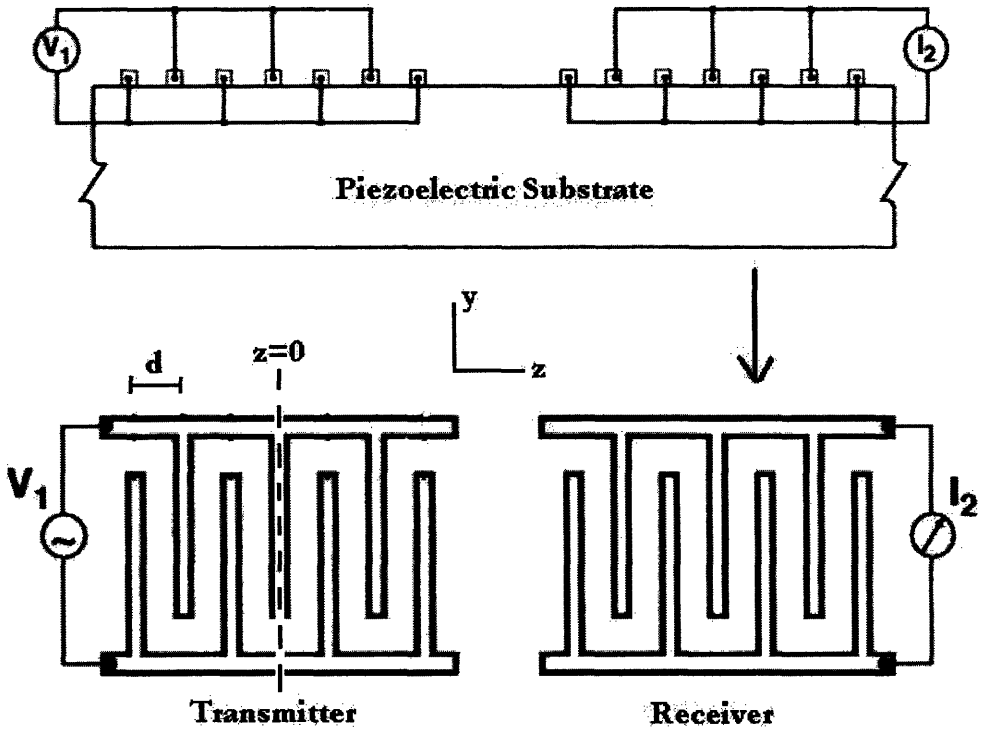

Figure 3-4: Structure of an IDT in a typical SAW device. Adapted from [18]

3.3 SAW Excitation and Detection

Surface waves are easily excited by lithographically patterning a pair of electrodes with interwoven fingers (each finger is separated from its neighbor by a distance d) onto a piezoelectric substrate. These electrode pair structures, known as interdigitated transducers (IDTs), are illustrated in Figure 3-4. We can excite the pieozoelectric crystal by driving the electrodes with an alternating voltage. The periodic electric field that results creates a standing wave with wavelength $\lambda_0 = 2d$ in the material directly underneath the IDT. This standing wave structure that our electric field forces on the material causes Rayleigh waves to emanate from either side of the IDT. Those propagating waves are produced most efficiently when we drive the device at its resonant frequency f_0, given by

$$f_0 = \frac{v_0}{\lambda_0}.$$

This resonant frequency corresponds to the frequency at which waves of the wavelength enforced by the IDT structure would naturally propagate through the material.

We detect the prescence of acoustic waves using the reverse piezoelectric effect. As mechanical vibrations occur under the surface of the receiver IDT when the Rayleigh wave passes, the electrical potential associated with that wave excites a current in the electrode that we read as the output signal of our device [17].

3.4 Frequency Response of IDTs

Each finger of an IDT can be thought of as a discrete source of acoustic waves, and we can model the electric potential of the wave radiated by finger n (with voltage V_n and location z_n) as

$$\phi^{\pm} = \mu_S V_n$$

where μ_S is a substrate-dependent constant and the + sign corresponds to a rightward propagating wave [18]. When we have an array of fingers, the contributions from each finger are additive. Therefore, a rightward traveling wave evaluated at position z can be described by

$$\phi^{+} = \mu_S \sum_{n=0}^{n=N_f-1} V_n e^{jk(z-z_n)}$$

where k is the familiar wave number related to the speed (v) and frequency (w or f) of the wave by $f = \frac{w}{2\pi} = \frac{vk}{2\pi}$. Now if we pick an arbitary reference axis that is in the middle of our symmetric IDT as shown in Figure 3-4, we find

$$\phi^{+} = \mu_S \sum_{n=0}^{n=N_f-1} V_n e^{-jkz_n}.$$

For our sensors where the finger spacing is a constant d and the voltages on successive fingers alternate according to $V_n = (-1)^n V_0$, the equation becomes more manageable:

$$\begin{aligned}
\phi^+ &= \mu_S V_0 \sum_{n=-\frac{N_f-1}{2}}^{n=\frac{N_f-1}{2}} (-1)^n e^{-jkdn} \\
&= \mu_S V_0 \sum_{n=-\frac{N_f-1}{2}}^{n=\frac{N_f-1}{2}} (-1)^n [\cos kdn + j \sin kdn] \\
&= \mu_S V_0 \sum_{n=-\frac{N_f-1}{2}}^{n=\frac{N_f-1}{2}} (-1)^n \cos kdn \\
&= \mu_S V_0 \sum_{n=-\frac{N_f-1}{2}}^{n=\frac{N_f-1}{2}} (-1)^n \cos\left(\frac{2\pi f dn}{v}\right) \\
&= \mu_S V_0 \sum_{n=-\frac{N_f-1}{2}}^{n=\frac{N_f-1}{2}} (-1)^n \cos\left(\frac{\pi f n}{f_0}\right) \\
&= \mu_S V_0 \left[1 + 2 \sum_{n=1}^{n=\frac{N_f-1}{2}} (-1)^n \cos\left(\frac{\pi f n}{f_0}\right)\right] \\
&= \mu_S V_0 \left[1 - 2\cos\left(\frac{\pi f}{f_0}\right) + 2\cos\left(\frac{2\pi f}{f_0}\right) + \ldots + 2(-1)^{\frac{N_f-1}{2}} \cos\left(\frac{N_f - 1}{2}\frac{\pi f}{f_0}\right)\right].
\end{aligned}$$

Rewriting this equation to see its behavior about the resonance frequency f_0:

$$\begin{aligned}
\phi^+ &= \mu_S V_0 \left[1 - 2\cos\left(\pi\frac{(f - f_0) + f_0}{f_0}\right) + 2\cos\left(2\pi\frac{(f - f_0) + f_0}{f_0}\right) + \ldots\right] \\
&= \mu_S V_0 \left[1 - 2\cos\left(\pi\frac{f - f_0}{f_0} + \pi\right) + 2\cos\left(2\pi\frac{f - f_0}{f_0} + 2\pi\right) + \ldots\right] \\
&= \mu_S V_0 \left[1 + 2\cos\left(\pi\frac{f - f_0}{f_0}\right) + 2\cos\left(2\pi\frac{f - f_0}{f_0}\right) + \ldots\right] \\
&= \mu_S V_0 \left[1 + 2 \sum_{n=1}^{n=\frac{N_f-1}{2}} \cos\left(\frac{f - f_0}{f_0}\pi n\right)\right].
\end{aligned}$$

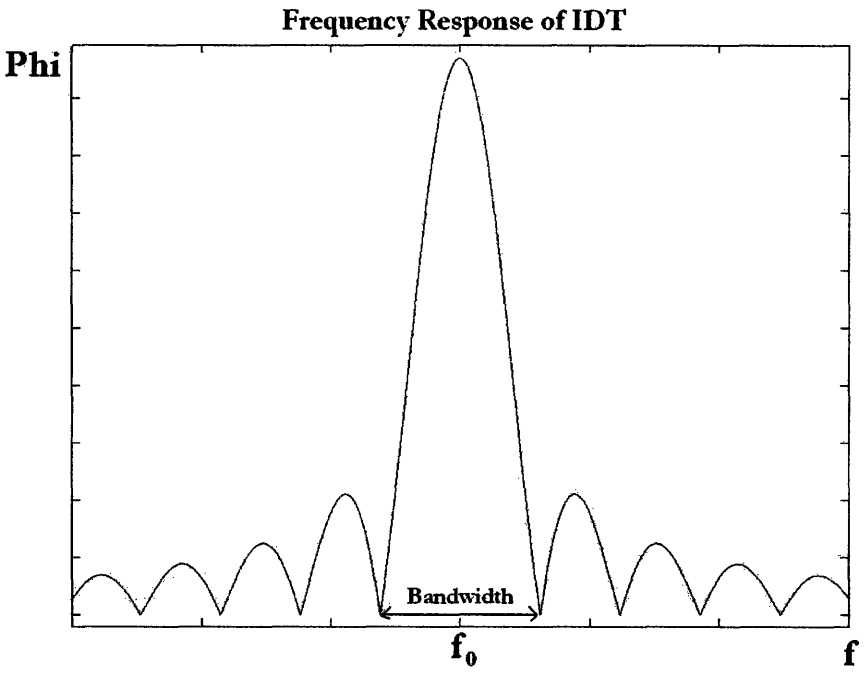

Figure 3-5: Frequency response characteristic of SAW device.

Plotting the last equation for a large number of fingers (in this case $N_f = 99$), we find the frequency response shown in Figure 3-5.

Graphing this equation for a few different N_f values, we find that the distance between nulls on either side of the IDT resonant frequency defines a bandwidth B that scales as

$$B \propto \frac{1}{N_f}.$$

This means that when we design our sensors we want to have a large number of fingers so that only a narrow band of frequencies is transmitted through our device.

3.4.1 SAW Perturbations

Interactions between the surface of the device and the Rayleigh wave are highly sensitive, which is what makes SAW devices such good sensors. Mechanical and/or

electric coupling between the substrate and the molecules sitting on its surface will change the velocity and attenuation properties of the acoustic wave [19].

Any traveling wave has a corresponding power density P (power/area) that is related to the wave's energy density U (energy/volume) by the velocity at which the wave travels: $P = Uv$. In a lossless medium, which we assume our substrate is for the most part, the power density remains constant during the propagation of the wave and we can relate changes in the wave energy density with changes in the wave velocity by differentiating:

$$\begin{aligned} P &= Uv \\ dP &= dUv + Udv \\ 0 &= dUv + Udv \\ \frac{dv}{v} &= -\frac{dU}{U}. \end{aligned}$$

3.5 SAWs as Biosensors for DNA Hybridization

When DNA strands hybridize to the functionalized surface of our sensor, the mass density on the surface increases and perturbs the waves propagating through our sensor. We need to calculate how sensitive our sensors will be to this type of perturbation. As an acoustic wave travels along the surface of our substrate in the x direction, it displaces particles according to [19]

$$\vec{u}(t) = \vec{u}e^{j(wt-kx)},$$

and the motion of these particles contributes to the kinetic energy density of the wave:

$$U_k = \frac{1}{2}\rho\sum_{i=1}^{3}\dot{u_i}^2.$$

Now consider how these equations are affected by the monolayer of DNA molecules that have been attached to the functionalized region of our devices. If we assume the layer moves in synch with the surface distortions, then the addition of the DNA molecules increases the kinetic energy density of the wave (by increasing the mass density on its surface) [19]. The kinetic energy changes even more when the layer of single-stranded DNA molecules is allowed to hybridize and further increase the surface mass density. The change in kinetic energy of the wave depends on the mass density of the new surface layer (ρ_S). Therefore, the change in average kinetic energy per unit surface area is just half the peak kinetic energy of all the particles on that surface[1]

$$dU_k = \frac{\rho_S}{4}\left(v_{x0}^2 + v_{y0}^2 + v_{z0}^2\right),$$

where v_{x0}, v_{y0}, and v_{z0} are the maximum particle velocities at the surface of the material when passing acoustic wave makes them go into their elliptical orbit [19]. Now to discover how much the velocity will be impacted by the prescence of the additional mass on the surface, we write

$$\begin{aligned}
\frac{dv}{v} &= -\frac{dU_k}{U} \\
&= -\frac{\rho_S}{4}\left(v_{x0}^2 + v_{y0}^2 + v_{z0}^2\right)\frac{1}{U} \\
&= -\frac{\rho_S}{4}\left(v_{x0}^2 + v_{y0}^2 + v_{z0}^2\right)\frac{v}{P} \\
&= -\frac{\omega v \rho_S}{4}\left(\frac{v_{x0}^2}{\omega P} + \frac{v_{y0}^2}{\omega P} + \frac{v_{z0}^2}{\omega P}\right) \\
\frac{dv}{v} &= -c_m f \rho_S
\end{aligned}$$

[1]Since waves slosh energy back and forth between potential and kinetic, the average kinetic energy density of a surface wave is just half its peak kinetic energy.

where c_m is the mass sensitivity factor given by

$$c_m = \frac{\pi v}{2}\left(\frac{v_{x0}^2}{\omega P} + \frac{v_{y0}^2}{\omega P} + \frac{v_{z0}^2}{\omega P}\right).$$

The $\frac{v_{x0}^2}{\omega P}$, $\frac{v_{y0}^2}{\omega P}$ and $\frac{v_{z0}^2}{\omega P}$ terms are actually independent of the input frequency and are a function of the material properties instead [19]. We expect to be able to fabricate SAW devices that operate in the GHz frequency range, so using values from [17] for the particle velocities we expect a sensitivity ($\frac{df_0}{d\rho_S}$) on the order of 100 Hz-μm^2/attogram.

Given this sensitivity level and the knowledge that DNA weighs 1x10^{-21} g / base-pair we can calculate the minimum number of nucleotide hybridizations that we can detect within a 400 μm^2 functionalized region:

$$\begin{aligned}\text{Num. of Nucl. Hyb.} &= \left(\frac{\text{1 nucleotide hybridization}}{\text{0.5E-21 g}}\right)\left(\frac{\text{1E-18 g}}{\text{100 Hz } \mu m^2}\right)(\text{3 Hz})(400\mu m^2) \\ &= \text{24000 nucleotide hybridizations.}\end{aligned}$$

3.5.1 Problems with Conventional SAW Biosensors

Conventional SAW biosensors detect the prescence of molecules on their surface by measuring the change in resonant frequency of the device (caused by the velocity change associated with the added surface mass) [30]. Although this kind of device is very sensitive and is widely used in different kinds of physico-chemical sensors, it has several limitations. For example, it is not a highly specific sensor - meaning any small change in the surface properties will shift the resonant frequency of the device. Ideally only the successful hybridization of DNA strands would shift the resonant frequency, but in typical SAW devices any particle on the surface of the device will change the properties of the acoustic wave. One of the major drawbacks of these SAW sensors is how difficult it is to distinguish noisy signals from the signals of the reaction being studied [30].

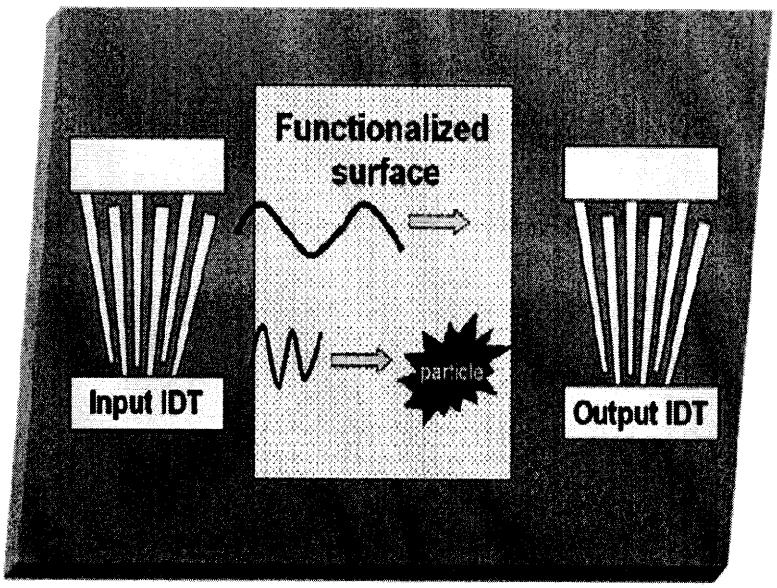

Figure 3-6: One-dimensional SAW device with tapered IDT.

3.5.2 Advantages of Tapered IDTs

Our novel SAW sensors use tapered IDTs as shown in Figure 3-6 that give us more information about the functionalized region of the sensor. These new devices should be much less susceptible to noise and have a number of interesting applications, including possible use as the detection mechanism for a quick, low-cost DNA microarray.

With tapered IDTs, the finger spacing (d_1) changes linearly across the transducer aperture. This means that the resonant frequency also varies across the device, so by controlling how we drive the input electrodes we can control what horizontal strip of the functionalized region we are sending the acoustic waves across. For example, when a rf signal with frequency f_1 is applied to the input electrode, an acoustic wave is launched in the small stripe of the electrode where f_1 x $(2d_1) = v_0$ is satisfied. Therefore, these new devices allow us to generate acoustic beams with spatial resolution.

As shown in Figure 3-6, the prescence of an unwanted particle on the surface of these new devices will only affect the acoustic signals whose frequency generates an acoustic path that interacts with the particle. The particle shown in Figure 3-7,

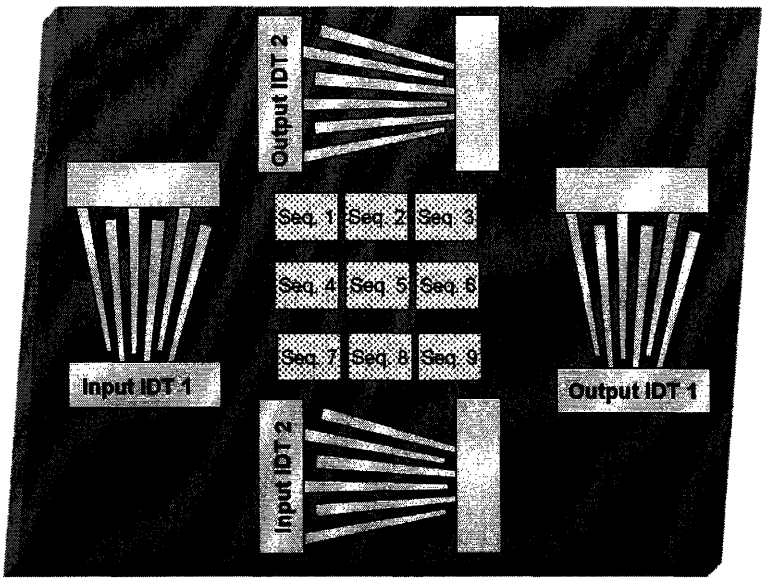

Figure 3-7: Two-dimensional SAW device with tapered IDT.

for example, will only affect the high frequency portion of the device signal leaving the low frequency portion intact. Properly calibrating these sensors should allow us to detect the prescence of an unwanted particle by observing how the output signal changes as a function of input frequency.

Expanding this idea even further, a pair of perpendicular tapered IDTs could be used as shown in Figure 3-7 to get two-dimensional spatial resolution in the sensing response. This type of sensor would not only provide huge improvements in noise reduction, but it could be the basis of a completely electronic DNA microarray.

3.5.3 Specifications of Our Devices

In this project, we fabricate several SAW devices so that we can perform a first-pass, proof-of-concept type experiment to demonstrate that they work as DNA hybridization sensors. The first device we designed was the basic SAW DNA-hybridization sensor shown in Figure 3-8. The image on top is from the CAD program we used to design the mask, while the images on bottom are actual photographs of the mask itself. We made the finger spacing as small as possible because the sensor will have the best resolution when the wavelength of the acoustic wave is as small as possible.

Figure 3-8: Basic SAW sensor.

The minimum feature size for our lithography equipment is 2.5 μm, so we chose that for our finger spacing. We chose to make each finger 2.5 μm thick as well for the same reasons. Combining this geometry with our material choice of GaN, the resonant frequency of our device should be approximately 370 MHz. Our mask also varies the number of fingers present in the five copies of this device (N_f = 20, 40, 60, 80, and 100). We chose a constant width of 160 μm and a constant length of 1000 μm, mainly because we wanted the width to be large enough to easy pattern DNA onto and the length we wanted to be 100 times the wavelength of the acoustic waves. As shown in these images, these devices have been designed with three connection pads 60 μm wide and 150 μm apart to allow us to perform RF measurements with a high frequency probe.

The second device we designed is a one-dimensional SAW sensor with tapered IDTs as shown in Figure 3-9. The image on top is again from the CAD program, while the images on bottom are of the mask itself. We have four copies of this device in our unit cell, two with 48 fingers and another two with 99 fingers. The bottom

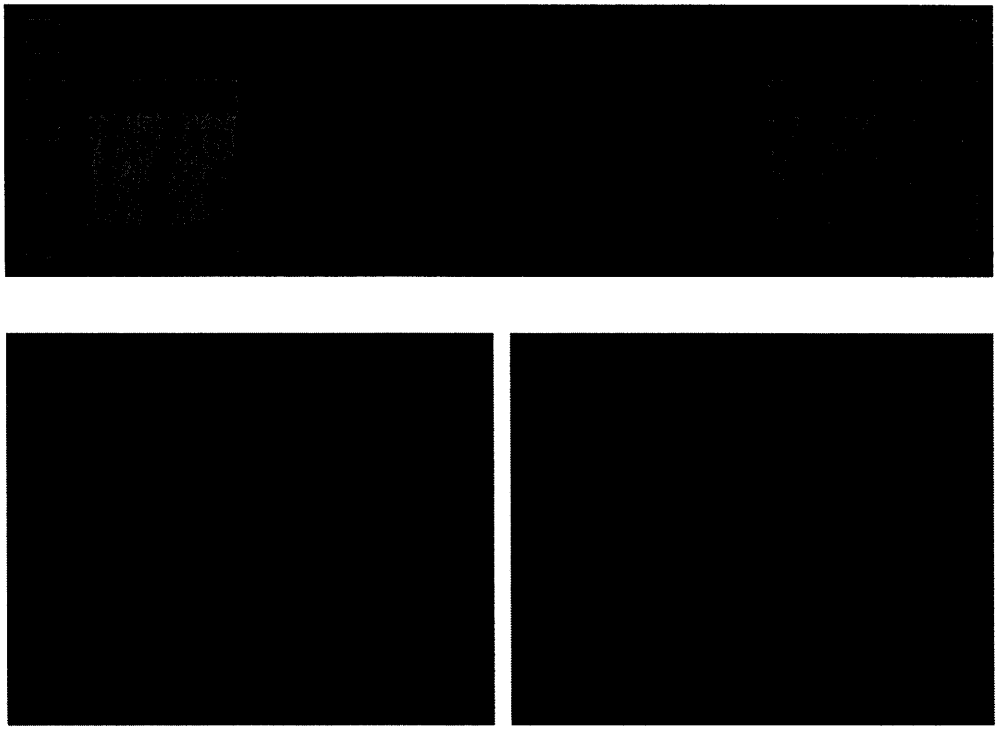

Figure 3-9: One-dimensional tapered SAW sensor.

crowded side of the device has the minimum finger spacing of 2.5 μm, while the top side has the fingers spaced 3 μm apart. The finger thickness is the same 2.5 μm throughout. This means that waves at the top of the device have a wavelength of 11 μm and waves at the bottom of the device have a wavelength of 10 μm. Given this 10% variation in wavelength across the aperture of the device, the frequency response of our 99-finger device should look like Figure 3-10. The three resonance peaks correspond to waves launched at the top, middle, and bottom of the device.

The third device we designed is a two-dimensional SAW sensor with tapered IDTs as shown in Figure 3-11. We have two copies of this device in our unit cell, one with 48 fingers and one with 99 fingers. The dimensions of each IDT are exactly the same as the one-dimensional version of this sensor.

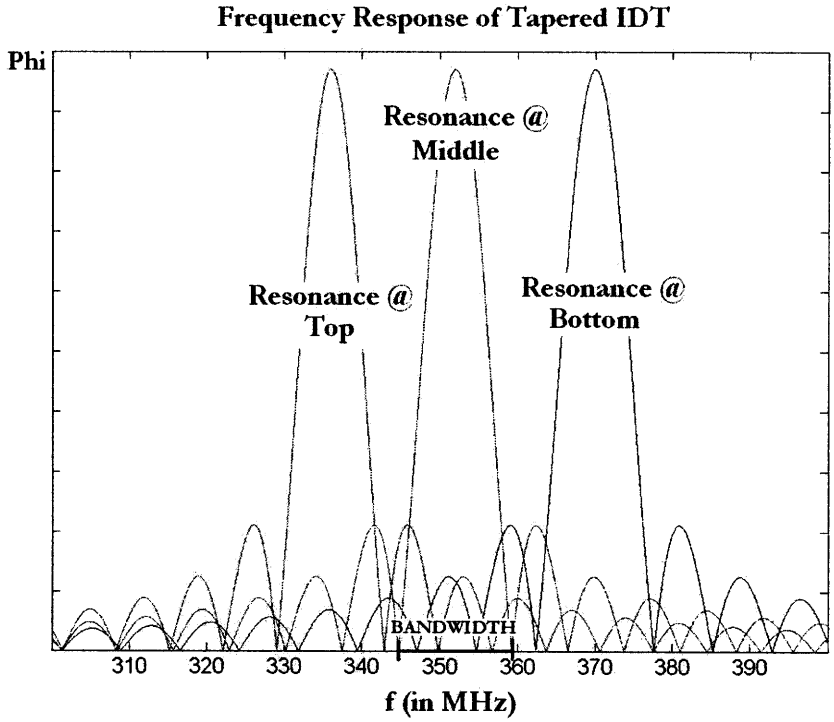

Figure 3-10: Frequency response of tapered IDT.

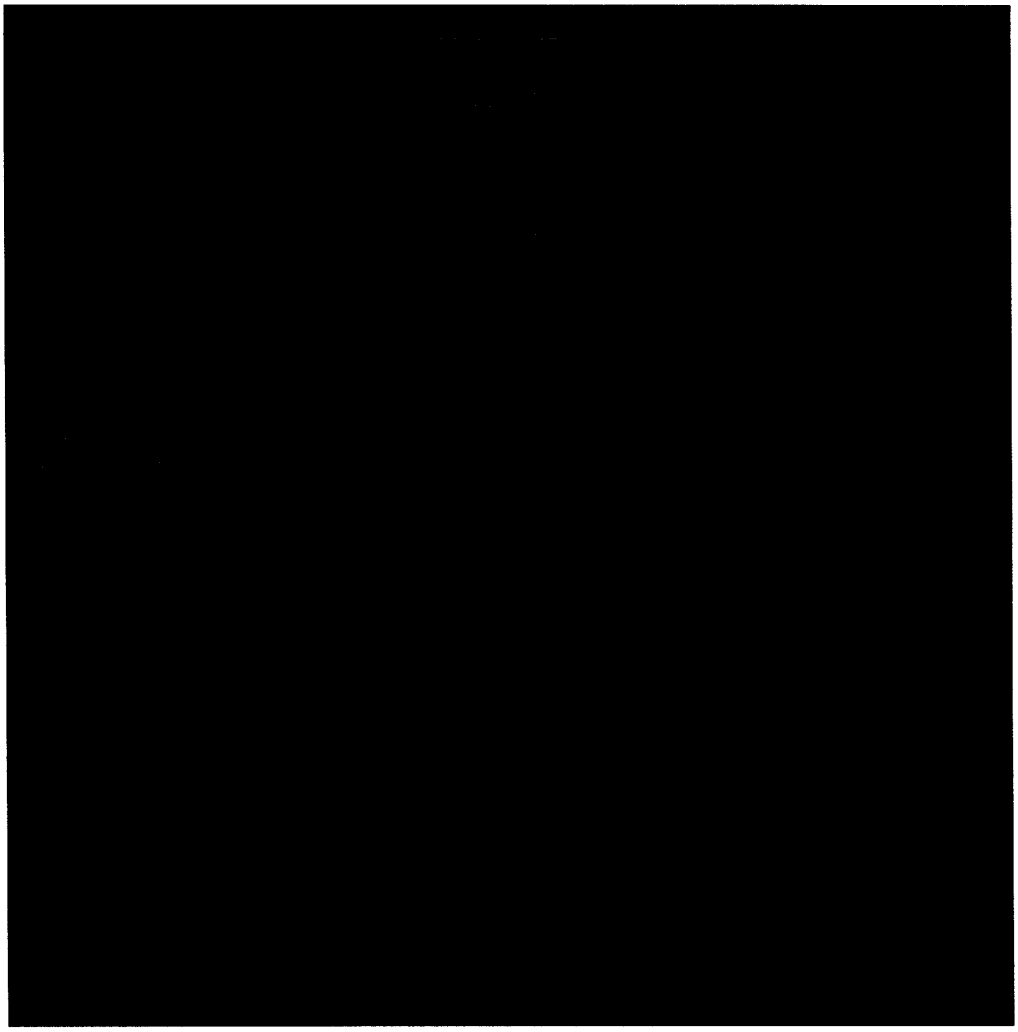

Figure 3-11: Two-dimensional tapered SAW sensor.

Chapter 4

Quantum Dot-Based Conductivity Sensor

4.1 Conventional Conductivity Sensors

Traditionally, conductivity sensors have tried to take advantage of the fact that the free flow of holes and electrons in a semiconductor depends to some extent on the what is happening at the interface between the semiconductor and the environment [22]. For example, if a large positive voltage is applied to the surface of a semiconductor, the electric field that results will draw electrons from the bulk of the crystal lattice towards the surface. These electrons are now available to conduct current near the surface of the semiconductor and as a result we see an increase in its conductivity.

The conductivity σ of a semiconductor can be described by

$$\sigma = q[\mu_e n + \mu_h p]$$

where q is the magnitude of the charge of a single electron, μ_e and μ_h are the electron and hole mobilities, and n and p are the concentration (number/volume) of electrons and holes in the semiconductor [23]. Because applying a positive voltage to the surface of a semiconductor linearly increases the number of electrons available for conduction,

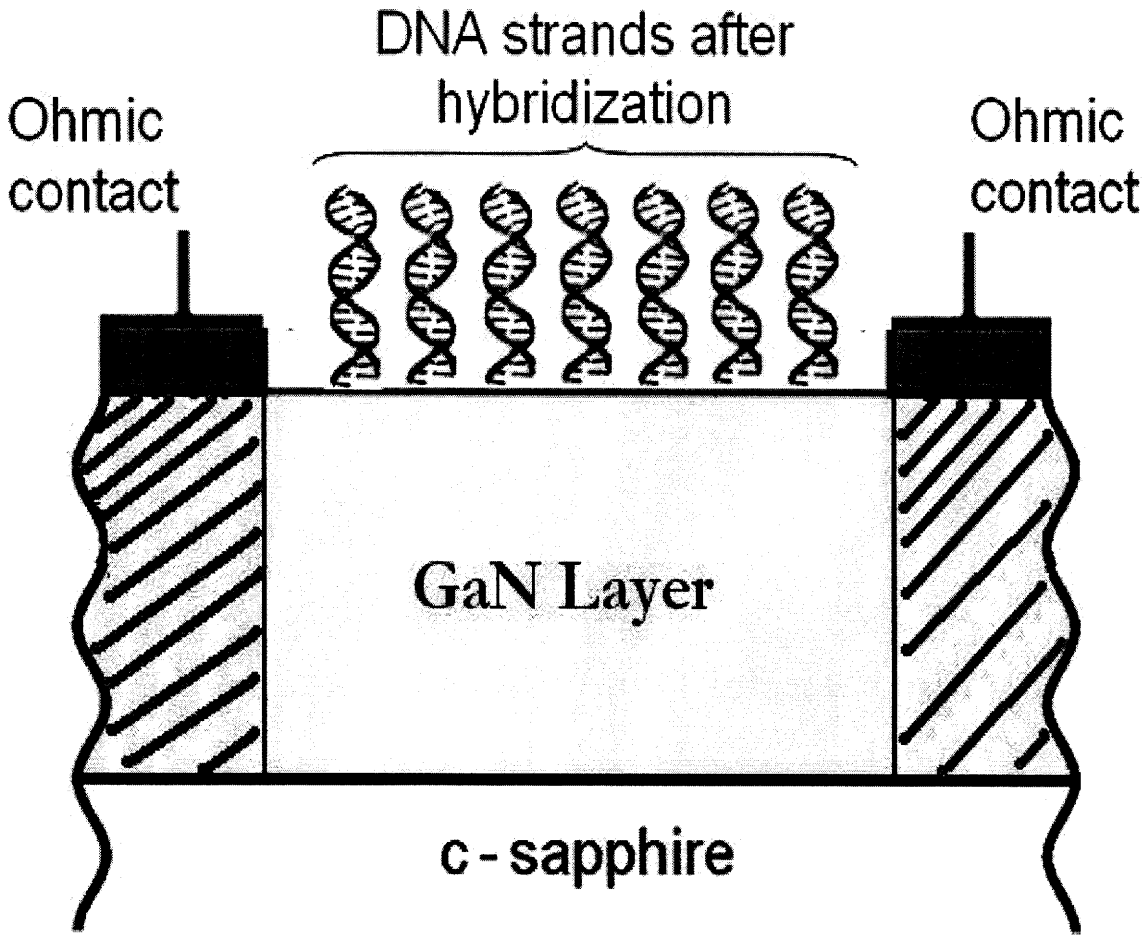

Figure 4-1: Structure of a basic conductivity sensor.

we also know that it will only cause a linear increase in the material's conductivity. This turns out be a serious limit on the sensitivity of these devices [31].

The conductivity of a substrate is easiest probed by lithographically patterning two ohmic contacts on the surface of the substrate, and then driving them some distance into the semiconductor with a high-temperature anneal. The resulting structure is depicted in Figure 4-1.

The performance of such a device depends on its geometry (the width, length, depth, and spacing of the ohmic contacts) and the properties of the underlying substrate. We can probe this sort of conductivity sensor by connecting one contact to

a voltage source and the other contact to ground, and then measuring how much current is able to flow through the semiconductor. The current flow will be described by the continuum form of Ohm's Law [23]:

$$\mathbf{J} = \sigma \mathbf{E}.$$

where J is the current density (current per unit area) and E is the electric field that the circuit imposes on the substrate between the ohmic contacts. A more convenient form may be

$$\begin{aligned} V &= IR \\ &= I\frac{L}{\sigma A}. \end{aligned}$$

This means that if we know the device geometry, we can easily calculate the measured conductivity [23]:

$$\sigma = \frac{I}{V}\frac{L}{HW}.$$

These conductivity sensors can be used to detect the hybridization of DNA when the surface of the semiconductor is functionalized as shown in Figure 4-1. Then when an analyte binds to the surface, it changes the net surface charge density which in turn affects the distribution of electrons and holes in the sample. The major limitation of this approach is really the limited sensitivity. It often takes a large number of molecules binding to the surface before there is any detectable change in the conductivity [31].

We can actually calculate the sensitivity of this type of sensor (assuming fabrication of a AlGaN/GaN HEMT-like structure without the gate) because the carrier

density in these semiconductors is typically 10^{12} cm^{-2}. Therefore, in a region 100 μm^2 we would need on the order of 10^6 electrons to double the carrier population and create a noticeable change in the conductivity. Since there is approximately 1 electron per nucleotide, this means the maximum sensitivity of this type of device would be about 1 million nucleotide hybridizations per 100 μm^2.

4.2 Quantum Dot Enhancement

We overcome the limited sensitivity of traditional conductivity sensors with a new design that uses the electronic properties of quantum dots as an amplification mechanism [24]. When quantum dots are present between the two ohmic contacts the primary conduction mechanism is known as variable range hopping conduction. It has been determined that variable range hopping conduction depends exponentially on electric field

$$\sigma \propto e^{-\sqrt{\frac{k_b T}{2qaE}}}$$

where k_b is the Boltzmann constant, q is the charge on an electron, and a is the localization length of the quantum dot [25]. Now when a hybridization event increase the net surface charge of the device, there will be an exponential increase in conductivity. In much the same way as our SAW sensors described in the previous chapter, this method of detecting DNA hybridization lends itself very well to the design of DNA microarrays. A two-dimensional array of ohmic contacts distributed around an appropriately functionalized region of quantum-dot enhanced semiconductor could be probed by a series of conductivity measurements to reveal a tomographic image of the surface.

To fabricate this sensor, we use a sample with epitaxially grown quantum dot layers as shown in Figure 4-2. Epitaxially growing the quantum dot layers should give us very precise control over the number of layers and density of quantum dots.

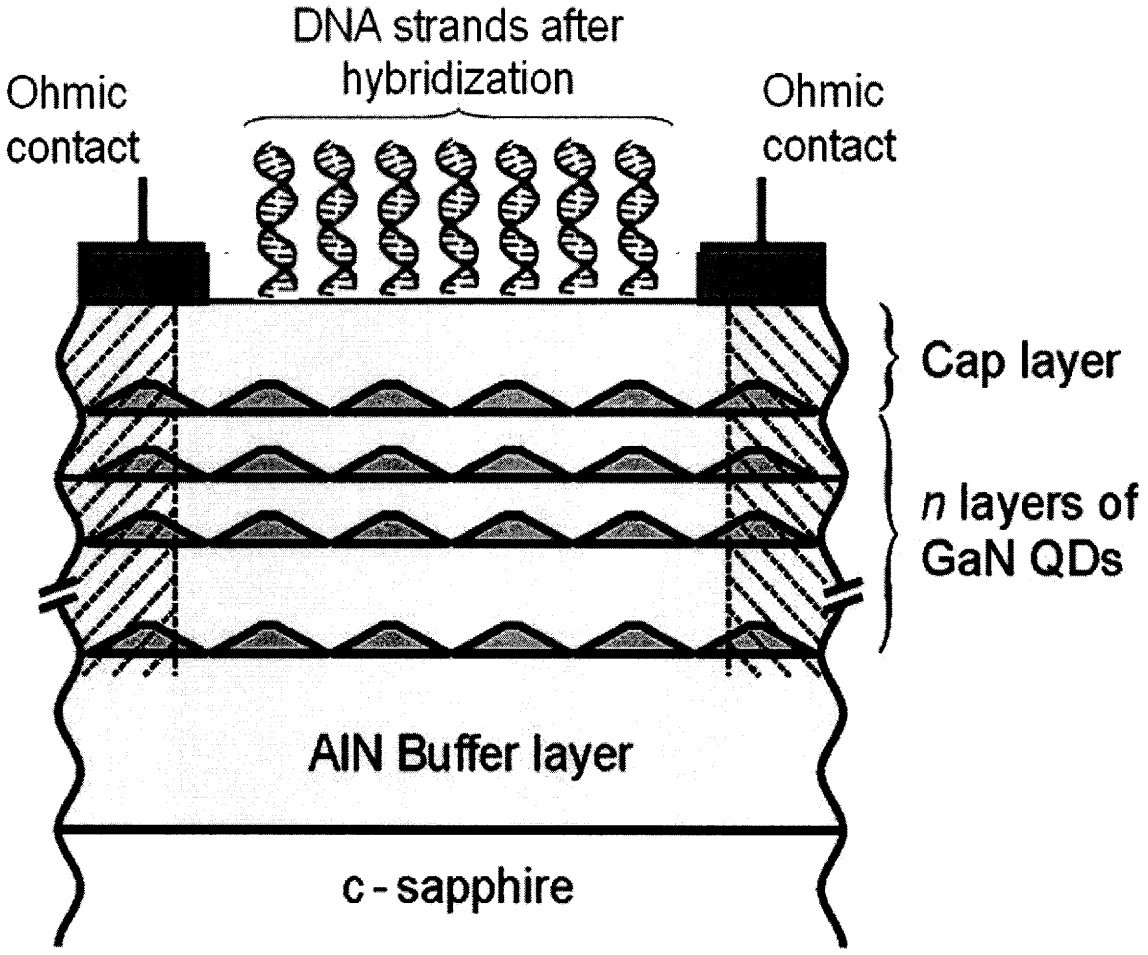

Figure 4-2: Structure of our epitaxially grown quantum dot-based conductivity sensor.

The photolithographic mask that we designed for creating these conductivity sensors is shown in Figure 4-3. Our unit cell contains sensors with several different sizes of ohmic contacts and several different separation distances between the ohmic contacts. This is so we can begin to make optimizations towards the optimal device geometry.

We also include other devices that we can compare the performance of our conductivity sensor against, including a Shottky diode in which we plan to pattern DNA onto the Schottky metal in the center circle shown in Figure 4-4. The image on left is from the CAD program, while the images on the right are of the mask itself. As shown in these images, these devices have been designed with three connection pads 60 μm wide and 150 μm apart to allow us to perform RF measurements with a high frequency probe.

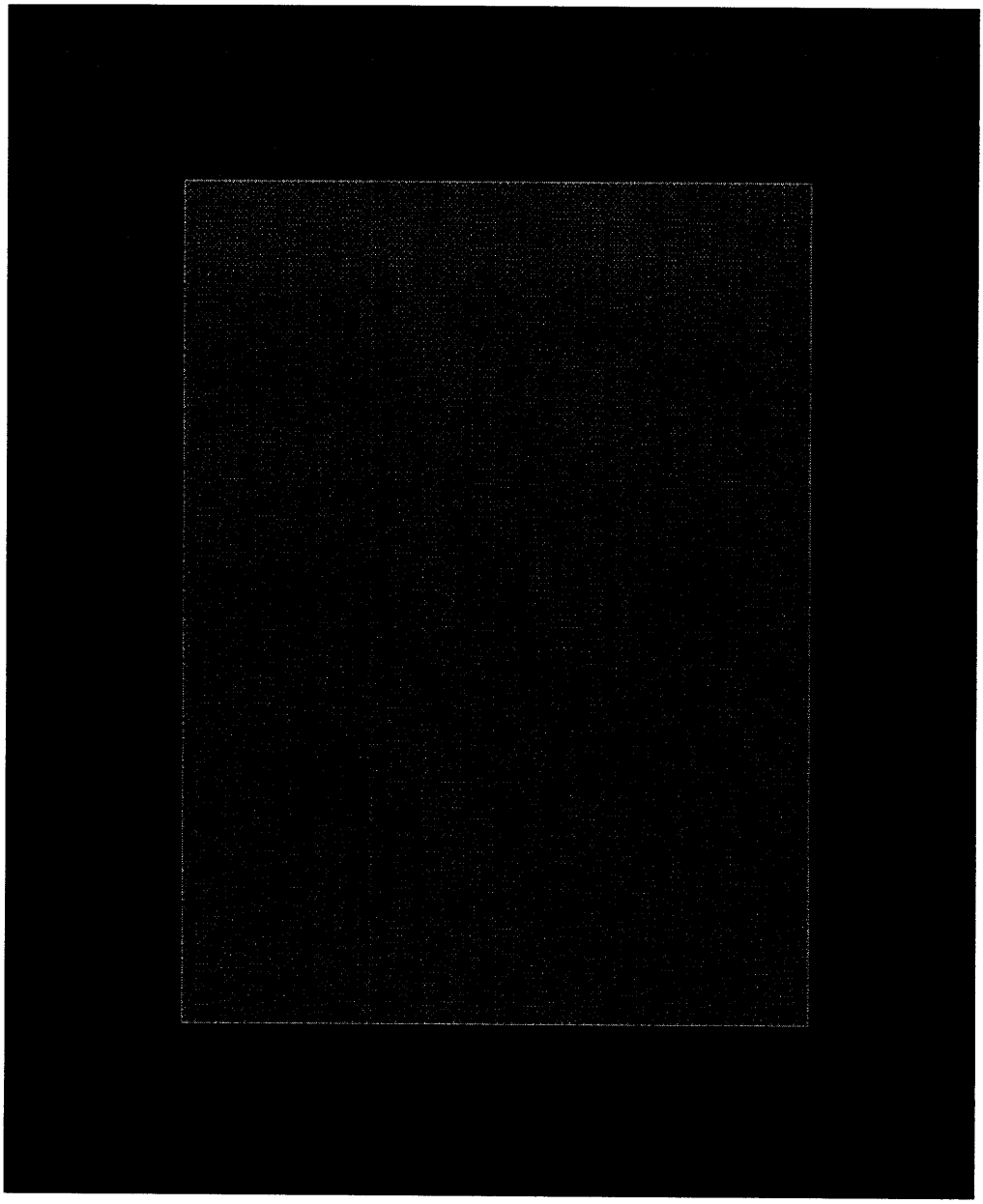

Figure 4-3: Conductivity sensor.

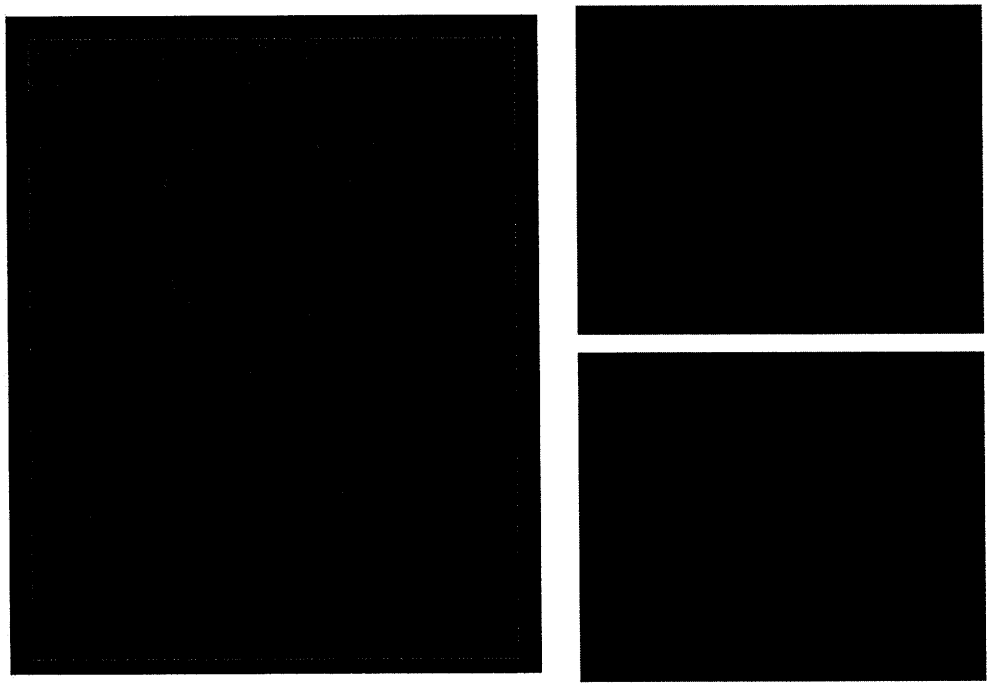

Figure 4-4: Shottky diode sensor.

Chapter 5

Transistor Sensors

GaN transistors have demonstrated a number of advantages over existing technologies, including an order of magnitude greater power density and improved efficiency [26]. Not only that, but they are easy to fabricate, chemically very stable, and - perhaps most importantly - not toxic to living cells. They are also optically transparent which opens the door for simultaneous electronic and optical methods of analysis [27]. For all these reasons there has been a lot of recent interest in using GaN transistors like the one shown in Figure 5-1 as biosensors.

5.1 Structure of a GaN HEMT Biosensor

The standard approach to turning a transistor into a biosensor is to functionalize the gate region, and let the potential change induced by the prescence or absence of the biomolecule regulate the flow of current through the device. This is the approach of famous ISFET [28, 29], and it has had some success but for maximize sensitivity these transistors must be operated very close to pinch-off levels where the subthreshold current flow changes exponentially with gate voltage. This is a problem because the low subthreshold current makes the output signal extremely sensitive to noise and temperature drift [28].

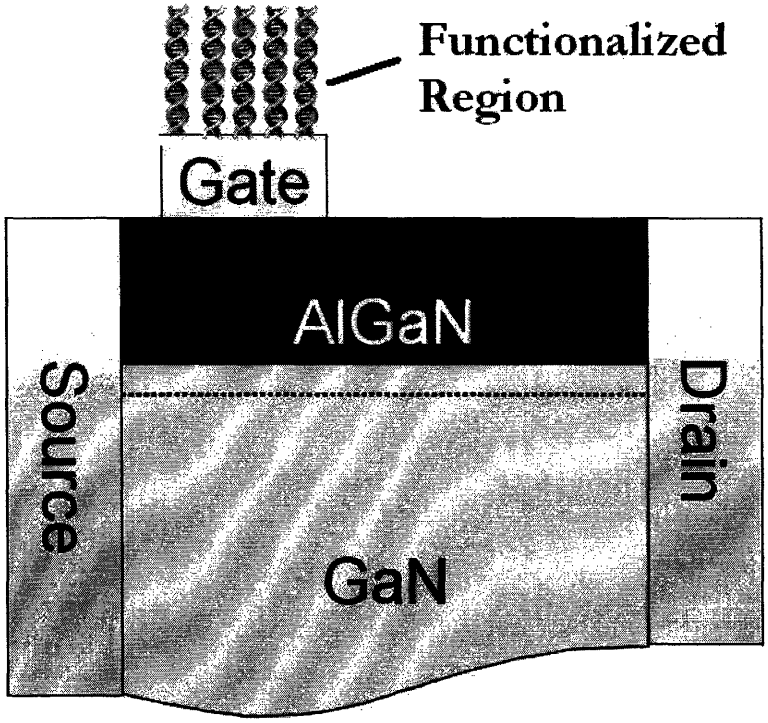

Figure 5-1: Basic structure of an AlGaN HEMT.

5.2 Drain Access Region Sensor

We have designed a new type of transistor biosensor that uses the drain access region for functionalization as shown in Figure 5-2. When hybridization events occur, they alter the charge density underneath the surface and create a linear change in the gate-to-drain capacitance of the transistor which we can detect as a change in the maximum switching frequency.

To better understand how to design this type of device, we look at the equivalent circuit shown in Figure 5-3. We can calculate the time constant for switching the transistor as

$$\tau_T = \frac{C_{gs}+C_{gd}}{g_m} + \frac{[C_{gs}+C_{gd}](R_s+R_d)}{g_m R_{ds}} + C_{gd}(R_s+R_d).$$

We also know that $\tau_T = \frac{1}{f_T}$ where f_T is the maximum frequency at which you can

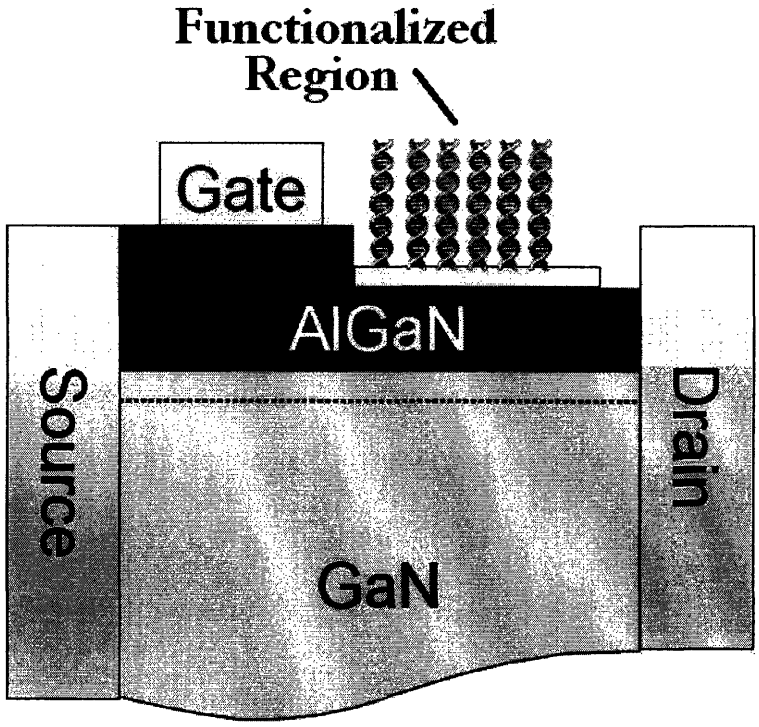

Figure 5-2: Basic structure of an parasitic capacitance-based HEMT biosensor.

turn on and off the transistor and still have current gain.

In order to maximize the sensitivity, we want to reduce the gate-to-source capacitance (C_{gs}) by making the gate length as short as possible [32]. Simulations have shown that current fabrication technologies can make C_{gd} almost the same as C_{gs}, which should allow even small changes in C_{gd} to affect the output frequency of our devices when they are plugged into an oscillator circuit [32].

In the fabrication of these sensors, we can control the following properties in order to improve the sensitivity:

1. Length of the gate (50 nm - 2500 nm).

2. AlGaN thickness (50 $\AA$ - 300 $\AA$).

3. Size of active region (5 μm - 100 μm).

4. Functionalization density.

Our photolithographic mask has several copies of the parasitic capacitance-based

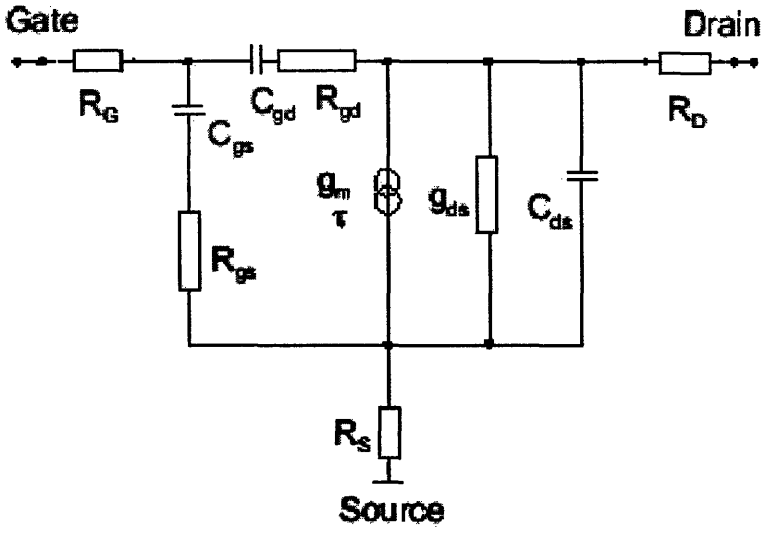

Figure 5-3: Circuit model for HEMT. Adapted from [32].

transistor sensor as shown in Figure 5-4. The image on top is again from the CAD program, while the images on bottom are of the mask itself. We used a gate length of 2.5 μm, leaving an area approximately 40μm by 400μm available for functionalization.

Our mask also includes a transistor sensor where the functionalization region is actually on the gate as shown in Figure 5-5, and it is mainly for comparison purposes.

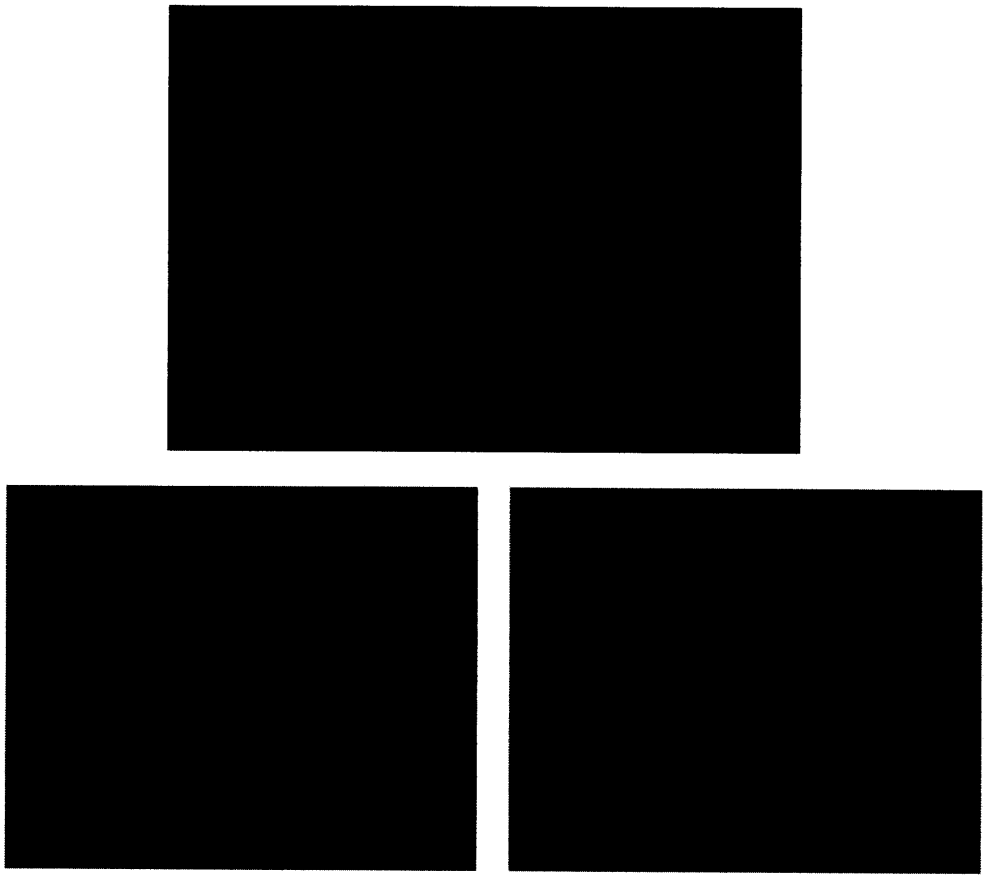

Figure 5-4: Parasitic capacitance-based transistor sensor.

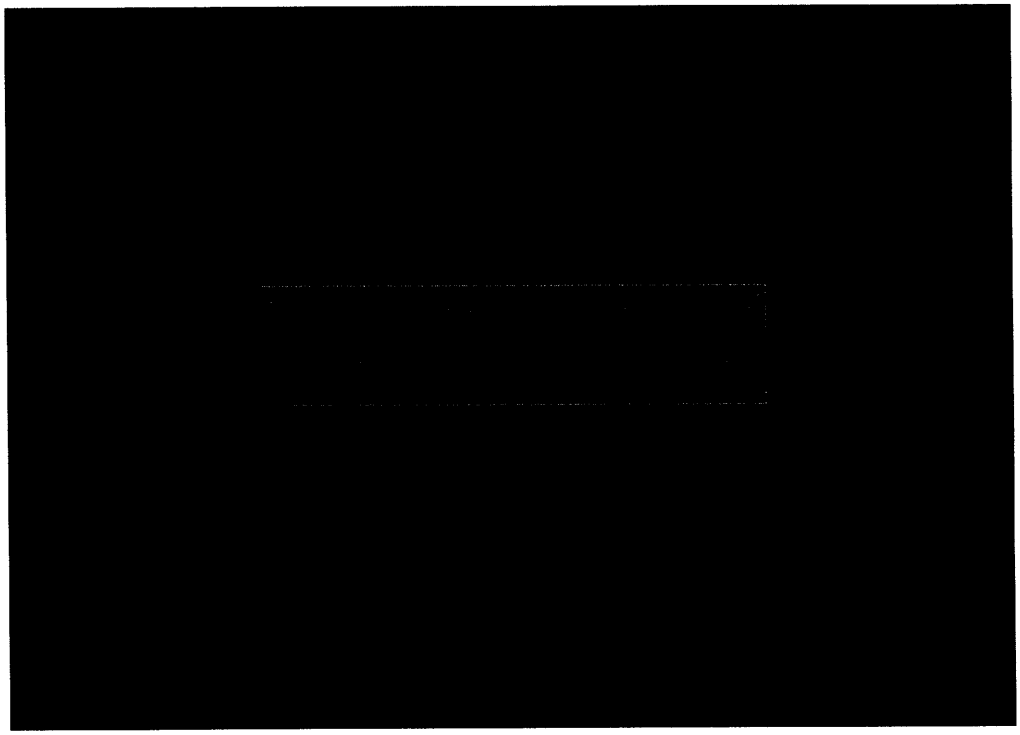

Figure 5-5: Gate active transistor sensor.

Chapter 6

Conclusion

Since this was only the first semester of this biosensor project, our main goals were to study the expected performance of the devices, optimize their design, define the process flow and begin the fabrication process. As a result, we spent most of our time studying/developing the devices, creating the photolithographic mask, and learning how to use the necessary fabrication facilities. In spite of time constraints, we have been able to make significant headway with this project, and are just a few weeks away from completing the fabrication and characterization of the SAW sensor.

This project shows promise as a stepping stone towards genetic analysis platforms that are faster and cheaper than those currently being used to sequence the human genome. Our approach takes advantage of the favorable properties of nitride semiconductors and uses novel detection schemes that should give our sensors more sensitivity and flexibility than anything currently on the market.

THIS PAGE INTENTIONALLY LEFT BLANK

Bibliography

[1] Nowicki, Stephen *Biology: The Science of Life: lecture notes,* (The Teaching Company Limited Partnership, 2004).

[2] Church, George M., "Genomes for ALL," *Scientific American,* (January 2006): 47–54.

[3] Cohen, Jon, "Sequencing in a Flash," *Technology Review,* (May-June 2007): 72–77.

[4] Shendure, J., Mitra, R.D., Varma, C., & Church, G., "Advanced Sequencing Technologies: Methods and Goals," *Nature Reviews: Genetics,* **volume**(5), (May 2004): 335–344.

[5] Purves, W.K., Sadava, D., Orians, G.H., & Heller, H.C., *Life: The Science of Biology,* Sixth Edition, (Sunderland, Massachusetts: Sinauer Associates, 2001): 320–322.

[6] Purves, W.K., Sadava, D., Orians, G.H., & Heller, H.C., *Life: The Science of Biology,* Sixth Edition, (Sunderland, Massachusetts: Sinauer Associates, 2001): 47–49.

[7] Purves, W.K., Sadava, D., Orians, G.H., & Heller, H.C., *Life: The Science of Biology,* Sixth Edition, (Sunderland, Massachusetts: Sinauer Associates, 2001): 202–206.

[8] Yu, A.A., Savas, T.A., Taylor, G.S., Guiseppe-Elie, A., Smith, H.I., & Stellacci, F., "Supramolecular Nanostamping: Using DNA as Moveable Type," *Nano Letters,* **volume**(5), **number**(6), (2005): 1061–1064.

[9] Baur, B., Steinhoff, G., Hernando, J., Purrucker, O., Tanaka, M., Nickel, B., Stutzmann, M., & Eickhoff, M., "Chemical functionalization of GaN and AlN surfaces," *Applied Physics Letters,* **volume**(87), (2005).

[10] Kang, B.S., Pearton, S.J., Chen, J.J., Ren, F., Johnson, J.W., et al., "Electrical detection of deoxyribonucleic acid hybridization with AlGaN/GaN high electron mobility transistors," *Applied Physics Letters,* **volume**(89), (2006).

[11] Ilic, B., Yang, Y., Aubin, K., Reichenbach, R., Krylov, S., & Craighead, H.G., "Enumeration of DNA Molecules Bound to a Nanomechanical Oscillator," *Nano Letters,* **volume**(5), **number**(5), (2005): 925–929.

[12] Williams, L.D., Maher, J.L., "Electrostatic Mechanisms of DNA Deformation," *Annu. Rev. Biophys. Biomol. Struct.,* **volume**(29), (2000): 497–521.

[13] Dessinges, M.N., Maier, B., Zhang, Y., Peliti, M., Bensimon, D., & Croquette, V., "Stretching Single Stranded DNA, a Model Polyelectrolyte," *Physical Review Letters,* **volume**(5), **number**(5), (2005): 925–929.

[14] Baumann, C.G., Smith, S.B., Bloomfield, V.A., & Bustamante, C., "Ionic effects on the elasticity of single DNA molecules," *Proc. Natl. Acad. Sci. USA,* **volume**(94), (2000): 6185–6190.

[15] Ballantine, D.S., et al., *Acoustic Wave Sensors: Theory, Design, and Physico-Chemical Applications,* (London, UK: Academic Press, 1997): 10–16.

[16] Ballantine, D.S., et al., *Acoustic Wave Sensors: Theory, Design, and Physico-Chemical Applications,* (London, UK: Academic Press, 1997): 22–31.

[17] Ballantine, D.S., et al., *Acoustic Wave Sensors: Theory, Design, and Physico-Chemical Applications,* (London, UK: Academic Press, 1997): 70–74.

[18] Ballantine, D.S., et al., *Acoustic Wave Sensors: Theory, Design, and Physico-Chemical Applications,* (London, UK: Academic Press, 1997): 74–78.

[19] Ballantine, D.S., et al., *Acoustic Wave Sensors: Theory, Design, and Physico-Chemical Applications,* (London, UK: Academic Press, 1997): 31–35 and 78–81.

[20] Streibl, M., Wixforth, A., Kotthaus, J.P., Govorov, A.O., Kadow, C., & Gossard, A.C., "Imaging of acoustic charge transport in semiconductor heterostructures by surface acoustic waves," *Applied Physics Letters,* **volume**(75), **number**(26), (1999).

[21] Palacios, T., Calle, F., Grajal, J., Monroy, E., Eickhoff, M., Ambacher, O., & Omnes, F., "High Frequency SAW Devices on AlGaN: Fabrication, Characterization, and Integration with Optoelectronics," *IEEE Ultrasonics Symposium,* (2002): 57–60.

[22] Yun, F., Chevtchenko, S., Moon, Y., Morkoc, H., Fawcett, T.J., & Wolan, J.T., "GaN resistive hydrogen gas sensors," *Applied Physics Letters,* **volume**(87), (2005).

[23] Fonstad, C.G., *Microelectronic Devices and Circuits,* (Mcgraw-Hill, 1994): 34–36.

[24] Yu, D., et al., "n-Type Conducting CdSe Nanocrystal Solids," *Science,* **volume**(300), (2003): 1277–1280.

[25] Yu, D., Wang, C., Wehrenberg, B.L., & Guyot-Sionnest, P., "Variable range hopping conduction in semiconductor nanocrystal solids," *Physical Review Letters,* **volume**(92), (2004).

[26] Mishra, U.K., Parikh, P., & Wu, Y., "AlGaN/GaN HEMTs - An Overview of Device Operation and Applications," *Proceedings of the IEEE,* **volume**(90), **number**(6), (June 2002): 1022–1031.

[27] Steinhoff, G., Purrucker, O., Tanaka, M., Stutzmann, M., & Eickhoff, M., "$Al_xGa_{1-x}N$ - A New Material System for Biosensors," *Advanced Functional Materials,* **volume**(13), **number**(11), (November 2003): 841–846.

[28] Bergveld, P., "Thirty years of ISFETOLOGY," *Sensors and Actuators B,* **volume**(88), (2003): 1–20.

[29] Steinhoff, G., Hermann, M., Schaff, W.J., Eastman, L.F., Stutzmann, M., & Eickhoff, M., "pH response of GaN surfaces and its application for pH-sensitive field-effect transistors," *Applied Physics Letters,* **volume**(83), **number**(1), (July 2003): 177–179.

[30] Barie, N., & Rapp, M., "Covalent bound sensing layers on surface acoustic wave (SAW) biosensors," *Biosensors and Bioelectronics,* **volume**(16), (2001): 979–987.

[31] Drummond, G.T., Hill, M.G., & Barton, J.K., "Electrochemical DNA sensors," *Nature Biotechnology,* **volume**(21), **number**(10), (October 2003): 1192–1199.

[32] Palacios, T., "Ph.D. Thesis," *University of California Santa Barbara,*.

[33] Parker, Ann, "Speeding the Gene Hunt:High-Speed DNA Sequencing," *http://www.llnl.gov/str/Balch.html,*.